JOURNAL OF combinatorial CHEMISTRY

Subscriber access provided by American Chemical Society

Article

Proteomimetic Libraries: Design, Synthesis, and Evaluation of p53–MDM2 Interaction Inhibitors

Felice Lu, Seung-Wook Chi, Do-Hyoung Kim, Kyou-Hoon Han, Irwin D. Kuntz, and R. Kiplin Guy

J. Comb. Chem., **2006**, 8 (3), 315-325• DOI: 10.1021/cc050142v • Publication Date (Web): 15 March 2006

Downloaded from http://pubs.acs.org on March 22, 2009

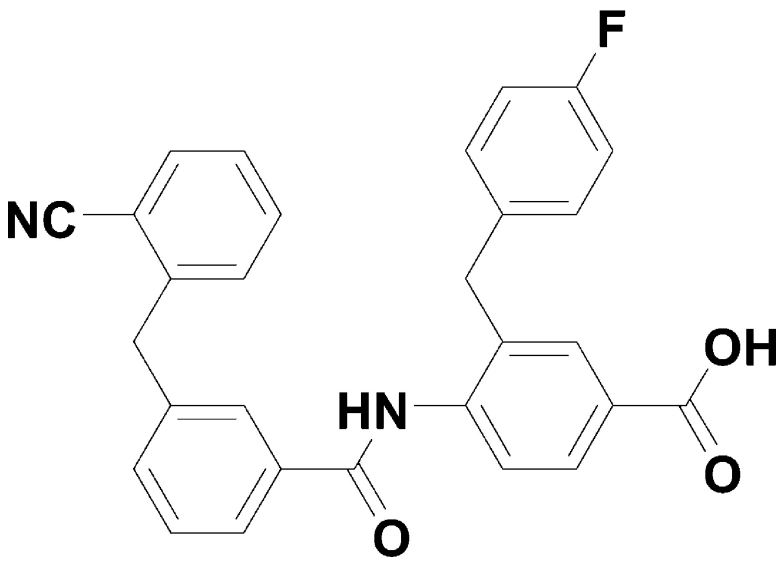

More About This Article

Additional resources and features associated with this article are available within the HTML version:

- Supporting Information
- Links to the 5 articles that cite this article, as of the time of this article download
- Access to high resolution figures
- Links to articles and content related to this article
- Copyright permission to reproduce figures and/or text from this article

View the Full Text HTML

ACS Publications
High quality. High impact.

Journal of Combinatorial Chemistry is published by the American Chemical Society.
1155 Sixteenth Street N.W., Washington, DC 20036

Proteomimetic Libraries: Design, Synthesis, and Evaluation of p53−MDM2 Interaction Inhibitors

Felice Lu,[†] Seung-Wook Chi,[‡] Do-Hyoung Kim,[‡] Kyou-Hoon Han,[‡] Irwin D. Kuntz,[§] and R. Kiplin Guy[§,⊥,*]

Chemistry and Chemical Biology Graduate Program and Departments of Pharmaceutical Chemistry and Cellular and Molecular Pharmacology, University of California, San Francisco, California, and Protein Analysis and Design Laboratory, Division of Drug Discovery, Korea Research Institute of Bioscience and Biotechnology, Yusong, P.O. Box 115, Daejon, Korea

Received October 17, 2005

The p53−MDM2 interaction regulates p53-mediated cellular responses to DNA damage, and MDM2 is overexpressed in 7% of all cancers. Structure-based computational design was applied to this system to design libraries centered on a scaffold that projects side chain functionalities with distance and angular relationships equivalent to those seen in the MDM2 interacting motif of p53. A library of 173 such compounds was synthesized using solution phase parallel chemistry. The in vitro competitive ability of the compounds to block p53 peptide binding to MDM2 was determined using a fluorescence polarization competition assay. The most active compound bound with $K_d = 12\ \mu M$, and its binding was characterized by ^{15}N-^{1}H HSQC NMR.

Introduction

Complex signal transduction networks involve series of protein−protein interactions, regulated by co-localization, coexpression, and control of the local physiochemical environment. These dynamic association events can be misregulated, leading to altered signaling responses often characteristic of cells in diseased states. The ability to manipulate these interactions holds the promise of a cure for diseases stemming from protein interactions gone awry. Antibodies, proteins, and peptides that inhibit protein−protein complexes exist, but many of these agents are plagued with poor bioavailability. Thus, identifying low-molecular-weight ligands that disrupt such protein−protein complexes remains an important problem.

In principle, protein binding interactions could be reproduced by small molecules in cases where small regions of a protein's binding surface account for the majority of the binding energy.[1] Efforts to mimic features of short peptides in extended or β-turn conformations have been quite successful.[2] However, only a handful of examples exist in which nonpeptidic small molecules mimic larger areas of protein surface such as one or more turns of an α-helix.[3−5] Much of the progress toward α-helix mimicry was reported by Hamilton and co-workers, who developed terphenyl derivatives as inhibitors of the interaction between CaM and smMLCK, Bak and Bcl-X_L, gp41 helical tertiary structures, and p53 and MDM2.[6−10] However, there is no general and reproducible method for the identification of such mimics. As part of our interest in helix surface recognition, we chose to use this outstanding problem as a test bed for the development of methods for scaffold and library design.

Although progress has been made in the design of enzyme inhibitors, it remains difficult to accurately predict the binding of small compounds to nonenzyme proteins, or to sites other than the active site of enzymes.[11] Some of the obstacles presented by protein−protein targets include flat nondescript binding interfaces and large bioactive surface areas. However, the binding energy is not usually distributed evenly over the large surface, leading to hot spots of binding composed of several residues in the protein interface.[12] Because hot spots serve as the optimal site for small molecule inhibition, we have chosen to target the p53−MDM2 complex, whose interface represents such a hot spot.[13]

The p53 gene encodes a tumor suppressor protein that controls a signaling pathway that protects cells from malignant transformation due to cellular stress such as DNA damage, hypoxia, certain cytokines, or other stimuli.[14] In the absence of such stressors, the activity of p53 is normally suppressed by the oncoprotein MDM2 through an autoregulatory feedback loop. Both inactivation of the p53 protein and overexpression of MDM2 have been associated with increased tumor incidence in human patients.[15] Therefore, activation of the p53 pathway via disruption of the p53−MDM2 interface has been considered an important therapeutic strategy. The crystal structure of MDM2 bound to a peptide from the transactivation domain of p53 reveals a small amphipathic α-helix bound to a relatively deep well-defined hydrophobic pocket of MDM2 (Figure 1A).[16] This pocket is filled primarily by Phe19, Trp 23, and Leu 26, the

* To whom correspondence should be addressed. Current address: Department of Chemical Biology and Therapeutics, St. Jude Children's Research Hospital, Memphis, TN 38103. E-mail: kip.guy@stjude.org.cgl.

† Chemistry and Chemical Biology Graduate Program, University of California.

‡ Korea Research Institute of Bioscience and Biotechnology.

§ Department of Pharmaceutical Chemistry, University of California.

⊥ Department of Cellular and Molecular Pharmacology, University of California.

10.1021/cc050142v CCC: $33.50 © 2006 American Chemical Society
Published on Web 03/15/2006

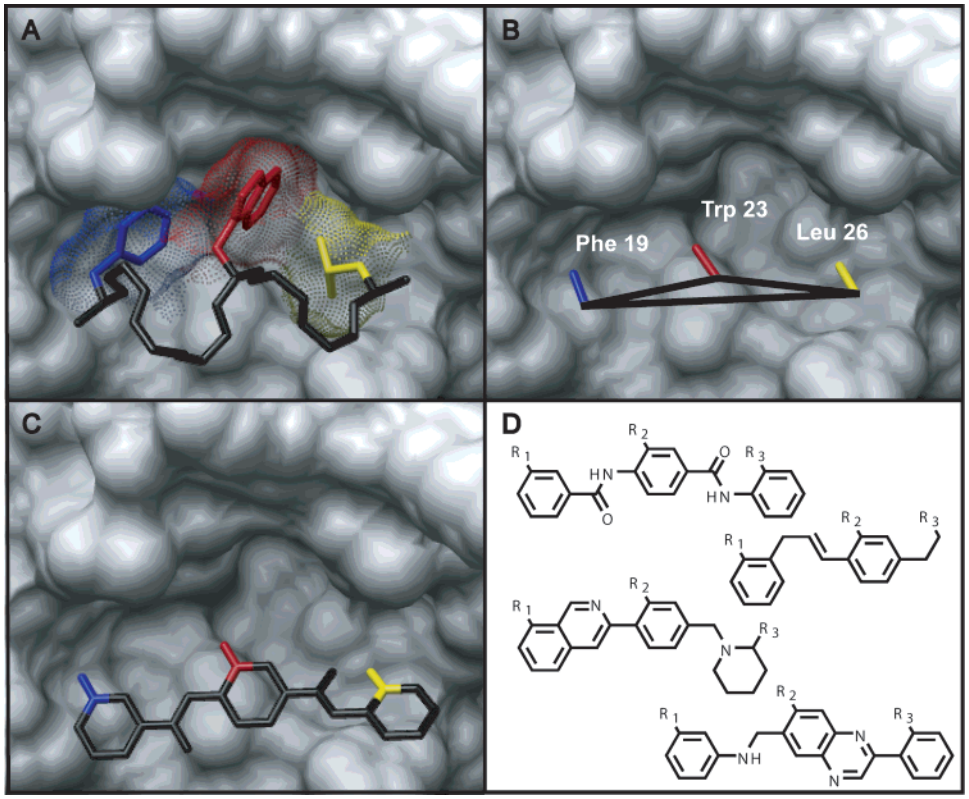

Figure 1. (A) Backbone trace of p53 peptide shown with MDM2.[16] Residues 19F (blue), 23W (red), and 26L (yellow) of p53 occupy a deep hydrophobic pocket. (B) Cα−Cβ bonds of 19F, 23W, and 26L used the CAVEAT search for scaffolds. (C) Library scaffold chosen for synthesis fulfills geometric requirements of CAVEAT search. (D) Structures of four compounds considered for synthesis.

i, *i* + 4, and *i* + 7 side chains from the hydrophobic face of the p53 α-helix. p53-based peptide libraries have produced compounds which inhibit the p53−MDM2 interaction in vitro and the expression of such peptides as fusion proteins activates p53 in vivo, thereby setting the stage for the small molecules to follow.[17,18]

In recent years, several chemical inhibitors of MDM2 have been reported, attesting to the importance of the target as well as the suitability of the p53−MDM2 interface for small molecule binding. The chemotypes of these nonpeptide inhibitors include (1) chalcones,[19,20] (2) piperazine-4-phenyl derivatives,[21] (3) chlorofusin,[22] (4) norbornanes,[23] (5) nutlins,[24] (6) sulfonamides,[25] (7) benzodiazepinediones,[26] (8) isoindolinones,[27] and (9) terphenyls.[10] The majority of the reported inhibitors of the interaction of p53 and MDM2 are very weak. By far the most potent and well-characterized p53−MDM2 inhibitors are the nutlins, identified by high-throughput screening at Roche. The optimized inhibitors in this series bound to MDM2 with a K_d of 90 nM in vitro and were shown to have antitumor activity in xenographic mouse models of human tumors. X-ray crystallography and NMR structures revealed that nutlins bind to the p53-binding site of MDM2, mimicking the p53 peptide to a high degree. The next most potent series is a set of benzodiazepinediones that have in vitro activity, with the most potent compound binding at 80 nM. Again a co-crystal structure indicates that the inhibitor binding mode mimics that of the p53 peptide in placement of its side chains.

Two of the nine classes of known inhibitors were discovered through design or computational screening—the norbornanes and the sulfonamides. A sulfonamide, with IC_{50} of 32 μM, was discovered after selection by UNITY pharmacophore searches of the NCI chemical database.[25] Not surprisingly, the three pharmacophores used were Phe19, Trp23, and Leu26 of the p53 peptide. Zao and co-workers also searched for the same pharmacophores using UNITY, and then docked the resulting compounds. They synthesized a series of norbornanes and found them active in several cell lines. The most potent MDM2 inhibitors discovered through design are the terphenyls, with a binding affinity of 200 nM. These inhibitors were originally designed as *i*, *i* + 3, *i* + 7 α-helix mimics binding to calmodulin.[10] Although the most potent p53−MDM2 inhibitors were discovered through screening, less potent inhibitors conceived through computational screening and design are highly significant because they embody a knowledge-based approach that has the potential to evolve into the lead discovery strategy of the future. This paper, representing our efforts in advancing the field of computational design, describes a method of selecting scaffold candidates for proteomimetic libraries and applies this method in the small molecule friendly p53−MDM2 system.

Results

Design of Proteomimetic Library. The structure of p53 and MDM2 revealed a deep hydrophobic binding interface in which the three amino acids of p53 at the protein interface are presented in a linear manner from the *i*, *i* + 4, and *i* + 7 positions of an α-helix (Figure 1A). The amino acid side chains interact with MDM2, while the p53 peptide backbone makes few contacts. Thus, the stable folded α-helical structure of a protein provides a scaffold from which side

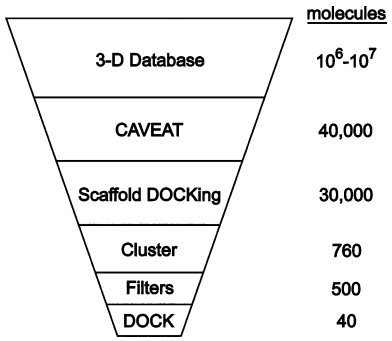

Figure 2. Overview of the multistep approach to library design.

chains are delivered to the binding pockets of MDM2. We approached the same problem by designing a nonpeptide molecule that can replace the peptide backbone while projecting side chain functionalities with distance and angular relationships equivalent to those seen in p53. A semirigid scaffold that can preorient side chains should facilitate binding by lowering the entropic penalty of ordering the backbone into a helical structure. Since the amino acid functionalities extend from the Cα−Cβ bond, the relative positions and orientations of three bonds will need to be present in the scaffold. This general scaffold search strategy can be applied to other types of helices as well as other protein motifs, providing a general approach for proteomimetics (Figure 2).

To find scaffolds that fulfill the geometric properties necessary for correct side chain placement, our design method employs CAVEAT.[28] CAVEAT searches through three-dimensional structure databases and returns molecules containing bonds with the same distance and angle relationships as those deemed critical in the reference structure. The MDM2-bound conformation of p53 served as the reference structure, and the Cα−Cβ bonds of 19F, 23W, and 26L of p53 were used (Figure 1B). To allow for uncertainty in the crystal structure side chain binding conformation, tolerances of 11° were used for bond angles and 0.24 Å were used for bond separations. A search of conformationally expanded versions of the ACD,[29] MDDR,[29] NCI,[30] CMC,[29] Iliad,[28] and Triad[28] databases yielded 40 000 structures that fulfilled the geometric requirements. Atoms extending beyond the Cβ equivalent positions were removed to allow side chains to be appended later in the design process.

Another important consideration in the scaffold design was creating chemical complementarity to MDM2. This factor was assessed using several rounds of scoring with DOCK 4.0[31](Figure 2). The computational time and design effort increased with each round, so it was important to remove poor scaffolds as early as possible using increasingly stringent scoring schemes. The DOCK ligand orientation function was not needed because CAVEAT had already oriented the ligand to match the corresponding bonds in the p53 reference structure. In the first round, no energy minimization was allowed and the score was based solely on van der Waals interactions. Scaffolds scoring greater than 1000 were deemed to have an irreparable clash with MDM2 and discarded from further consideration. The surviving structures were hierarchically clustered using two-dimensional Daylight fingerprint descriptors, a closest linkage algorithm, and a 0.85 Tanimoto coefficient.[32] Because fingerprint descriptors recognize chemical diversity, all heteroatoms were changed to carbon to effect geometric, rather than chemical, clustering. This resulted in 761 clusters.

Between the first and second rounds of DOCK scoring, several filters were used to remove poor scaffolds. Structures with no rings or greater than five consecutive rotatable bonds were removed in order to provide a conformationally rigid scaffold. Because strained or complex molecules would lead to difficult synthetic routes, molecules with three- or four-membered rings or more than three fused rings were also discarded. The application of these filters left 500 remaining clusterheads, which were minimized using DOCK 4.0 scored with a van der Waals scoring function. In this step, the ligand geometry was allowed to move with respect to the MDM2 target. Conformational variances and heteroatoms were restored to the molecules scoring in the top half, yielding 1369 three-dimensional structures.

At this point, the scaffolds alone could not be further distinguished by DOCK because the most important aspect of the interaction, the side chains, was missing. Hence, phenylalanine, phenylalanine, and leucine side chains were added to the R_1, R_2, and R_3 positions on the scaffold, corresponding to the 19F, 23W, and 26L positions of p53. The structures were evaluated with a van der Waals and electrostatics score using DOCK 4.0. Thus, the side chains aided in scaffold evaluation. The top 40 structures were visually inspected for synthetic accessibility. The main advantage of the selected scaffold (Figure 1C,D) was that it could be synthesized in a modular fashion with simple, seemingly straightforward chemistry. The only disadvantage was its high hydrophobicity, which could be addressed by replacing scaffold carbons with heteroatoms and by attaching hydrophilic functionalities to the solvent-facing side of the scaffold in later generations of molecules.

Theoretically, the selected scaffold with phenylalanine, tryptophan, and leucine side chains should bind to MDM2 with similar or greater affinity than the p53 peptide. There was also potential for increasing the binding affinity by optimizing side chain contacts. Previous experience demonstrated the difficulty and time required to accurately predict the binding of minor variations in side chains, so we decided to optimize side chains empirically rather than theoretically[33] (Chart 1).

Synthesis of Proteomimetic Library. The library members were composed of six parts—three scaffold aryl rings connected by amide bonds, and three side chains connected by carbon−carbon bonds. We envisaged synthesizing the library in solution (Scheme 1). We considered assembling the scaffold first, but thought there would be great difficulty in attaching three different side chains selectively. Therefore we decided to add side chains to each of the three aryl rings, and then use amidations to connect the individual subunits. An advantage of this strategy was the utilization of a common chemistry for production of diversity elements—Suzuki couplings were used to add side chains to each monomer at the diversity points. Carboxylic acid and amino groups were protected as methyl ester, formyl, and nitro groups during the production of diversity reagents.

Chart 1. Side Chains Chosen for Synthesis

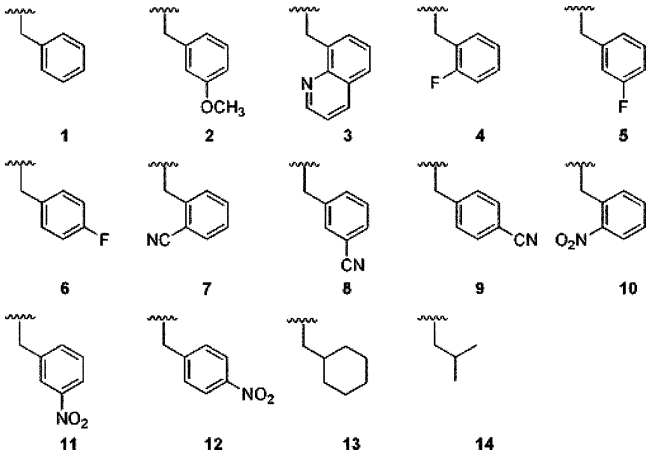

Scheme 1. Synthesis of Peptidomimetics: Synthesis of (A) Diversity Elements and (B) Library[a]

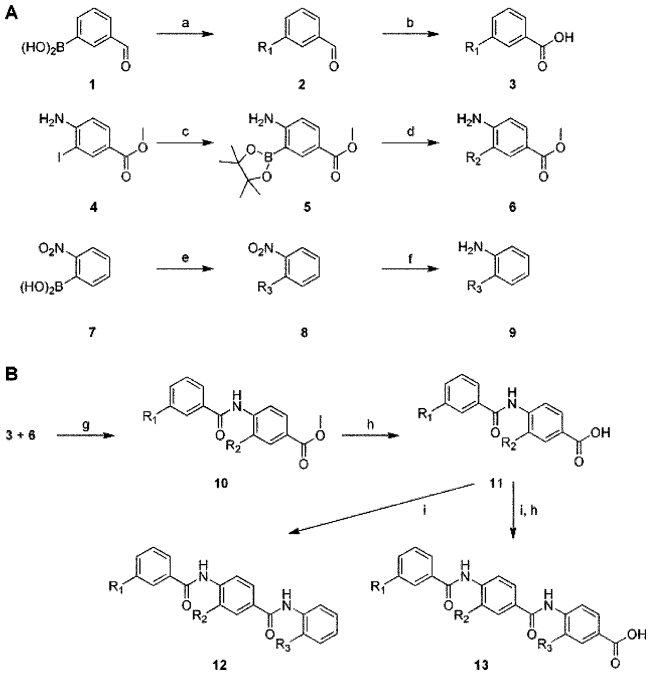

[a] Reagents and conditions: (a) R_1Br, $Pd(PPh_3)_4$, THF, K_2CO_3, 80 °C; (b) $NaClO_2$, NaH_2PO_4, H_2O_2, CH_3CN, 4 °C to room temperature; (c) pinacolborane, 1,4-dioxane, Et_3N, $PdCl_2$(dppf), 80 °C; (d) R_2Br, $Pd(PPh_3)_4$, THF, K_2CO_3, 80 °C; (e) R_3Br, $Pd(PPh_3)_4$, THF, K_2CO_3, 80 °C; (f) Pd/C, H_2; (g) PS-TsCl, DMAP, CH_2Cl_2, 40 °C; (h) NaOH, 1,4-dioxane; (i) PS-TsCl, DMAP, DMF, 40 °C.

Chemsets **2** and **8** were easily synthesized with 30−85% yield from commercially available reagents **1** and **7**, respectively.[34] The reactions proceeded cleanly, as the purity of the crude reaction was greater than 80% when analyzed by thin layer chromatography (TLC). Reduction of **8** by catalytic hydrogenation with palladium on carbon proceeded quantitatively in all cases. The oxidation of **2** was carried out using sodium chlorite as a mild oxidant and hydrogen peroxide as a scavenging agent for the hypochlorite byproduct.[35] Yields ranged from 60 to 100%, and the purity of the crude material was greater than 80% by TLC.

Synthesis of chemset **6** was more problematic. The initial strategy involved the synthesis of a benzaldehyde analogue of **5** via nitration of 3-formylphenylboronic acid.[36] Despite careful optimization all attempts yielded proteodeboronylated nitrobenzaldehydes and large amounts of starting material. Nitration of a more activated substrate, 3-hydroxymethylphenylboronic acid, yielded an inseparable mixture of nitroboronic acid regioisomers. Because of this regioselectivity problem, we developed a new approach starting from commercially available trisubstituted benzene **4**.

The synthesis of pinacolboronate **5** was based on conditions reported by Baudoin et al. for the synthesis of pinacol (2-aminophenyl)boronate from 2-bromoaniline.[37] Their optimal conditions employing palladium acetate as a catalyst and a biphenylphosphine ligand worked poorly for our substrate. However, conditions employing palladium chloride diphenylphosphinoferrocene, suboptimal in their case, resulted in 20% yield of **5**. The low yield can be partially attributed to product loss during silica chromatography. The subsequent Suzuki coupling to form **6**{*1*} proceeded smoothly under the conditions of Klarner et al. To prevent the significant product loss from silica purification of **5**, the boronate synthesis and Suzuki coupling were performed consecutively in one pot, increasing the yield for the two reactions to 35%.

Initial studies using standard coupling reagents for formation of an amide bond, such as DCC or oxalyl chloride, gave low yields and a multitude of side products. However, amide bond formation between each of the diversity elements was easily carried out under the conditions optimized by Soloshonok and co-workers for sterically hindered poorly nucleophilic amines.[38] Treatment of the acid component with tosyl chloride followed by addition of the aniline gave a clean reaction with good yield. Furthermore, the reaction conditions were easily adapted for parallel synthesis in 48-well FlexChem reaction blocks. The FlexChem's fritted reaction well facilitated the use of resin-bound tosyl chloride reducing the number of species in the crude product.

Proofing reactions for the synthesis of **3**, **6**, and **9** were carried out using side chain 1. Purified yields were greater than 75% for all reactions except c and d. The synthesis of chemsets **3**, **6**, and **9** followed with similar results. The exception was the nitro side chain, whose presence reduced the yield in Suzuki couplings by about half. Half-gram amounts of chemsets **3**, **6**, and **9** were synthesized and used as needed for library synthesis. The library synthesis reactions g−i were tested with methyl side chains. While test reactions proceeded quantitatively, the conversion time was longer for the actual side chains.

The size of the first production library of chemset **12** was limited to roughly 100 total members to ease handling. The side chains chosen were based on commercial availability and structural similarity to the phenyl side chain used in the proofing reactions (Chart 1). Preliminary calculations with the DOCK scoring function did not clearly favor one aromatic side chain over another, with one exception—saturated side chains such as cyclohexane scored poorly. Thus, side chain 13 was included in the list of diversity elements as a control for the efficacy of DOCK in predicting relative affinities in this case. The tryptophan side chain was not included because its reactivity rendered it synthetically intractable without addition of a protecting group. With three diversity elements and roughly 10 possible side chains for

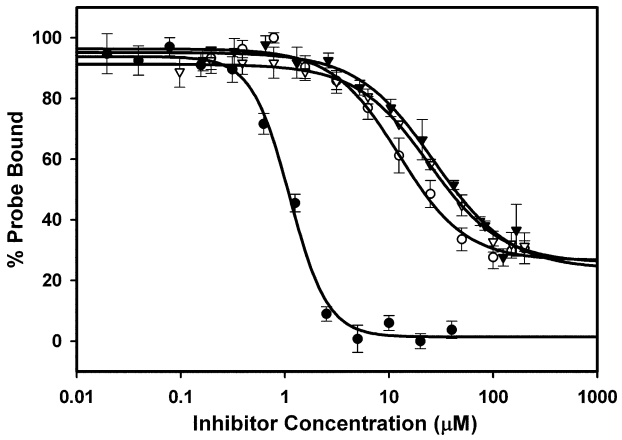

Figure 3. Competition of fluorescein-p53 by nutlin-3 (▽, K_d = 1.1 μM), **11**{*7,6*} (▼, K_d = 12 μM), **11**{*8,9*} (○, K_d = 24 μM), **11**{*5,9*} (●, K_d = 27 μM).

each diversity element, an all-by-all-by-all library would contain over a thousand compounds. Instead, 13 random combinations of chemset **10** were synthesized and converted to chemset **11**. Chemset **11** was coupled to nine R_3 elements to form chemset **12** for a total of 117 compounds. Members of chemset **11** were also tested for activity.

Assay of Biological Activity of Proteomimetic Library. The library was initially tested using a biochemical model for the interaction of p53 and MDM2 based on fluorescence polarization. This was implemented as a competition experiment using a fluorescently labeled p53 peptide of 19 amino acids in length and a recombinant $(His)_6$-tagged MDM2 protein expressed in *Escherichia coli*. Binding studies of the fluorescently labeled peptide show saturable binding with a K_d of 1.6 μM, which is in agreement with the literature value.[39,40] The validity of the assay was established with several controls: a positive control consisting of nutlin-3, and a negative control consisting of a peptide similar to the p53 probe containing alanine substitutions at 19F, 23W, and 26L. Using this assay, the entire library was screened at a fixed concentration of 30 μM. Compounds showing an inhibitory ability were then subjected to dose−response analysis. The binding curves for compounds with a binding constant of 30 μM or less are shown in Figure 3.

Because 3 of the 13 compounds in chemset **11** were active (Figure 4), we synthesized a second library focused on chemset **11**. The all-by-all library of chemset **11** was aimed at probing SAR and increasing potency. We also synthesized a few members of chemset **13**{*7,6,X*} to test the importance of the carboxylic acid functionality. This second library yielded a large number of weakly binding compounds with K_d greater than 30 μM (Table 1).

Table 1. Active Compounds

compd	K_i (μM)	compd	K_i (μM)
11{*7,6*}	12	**11**{*1,11*}	>30
11{*8,9*}	24	**13**{*7,6,8*}	>30
11{*5,9*}	27	**13**{*7,6,5*}	>30
11{*4,4*}	>30	**13**{*7,6,2*}	>30
11{*6,9*}	>30	**11**{*5,6*}	>30
11{*6,6*}	>30	**11**{*5,7*}	>30
11{*1,6*}	>30	**11**{*1,9*}	>30
13{*7,6,7*}	>30	**11**{*5,8*}	>30
11{*4,9*}	>30	**11**{*1,8*}	>30
11{*8,8*}	>30	**11**{*7,4*}	>30
11{*5,11*}	>30		

Characterization of Binding by NMR. To characterize the binding of **11**{*7,6*} on MDM2, we performed an NMR titration study on ^{15}N-labeled MDM2 (3−109) with the compound. Figure 5 shows the chemical shift perturbation in MDM2 residues upon binding of **11**{*7,6*} and the location of the significantly perturbed residues on the MDM2 surface. The most significantly perturbed MDM2 residues are Glu25, Phe55, His73, and Val93 (Figure 5A). All of these residues are located within the p53 helix-binding pocket of MDM2, indicating that **11**{*7,6*} binds to the p53-binding pocket in MDM2 (Figure 5B).[16] Therefore, **11**{*7,6*} is expected to competitively block p53 binding to MDM2. Interestingly, binding of **11**{*7,6*} and the p53 helix differentially influences the MDM2 residues within the same binding pocket. The **11**{*7,6*} affects amide proton resonances in the following order, His73 > Phe55 > Glu25 ≅ Val93, whereas for the p53 helix, His73 > Val93 > Tyr100 > Ser22. Therefore, the exact binding modes of the compound and the p53 helix might be slightly different from each other, although both bind to the same helix-binding pocket.

Discussion

We have constructed inhibitors of the p53−MDM2 interaction using a computational design strategy that can be applied to any protein−protein interaction for which a co-crystal structure exists. These inhibitors have a novel structure and represent a complementary approach to the screening methods used in the discovery of previous inhibitors. Because the inhibitor scaffolds were designed as α-helix mimics, the compound libraries may have activity in other protein−protein interactions in which an *i*, *i* + 4, *i* + 7 α-helix plays a role. Within a library, side chains dictate protein specificity. Some of these proteins include but are not limited to Bak, NF-κB, and VP16. The success of the libraries in these other systems will speak toward the extent of their α-helix mimicry as will the synthesis and testing of the remaining scaffolds.

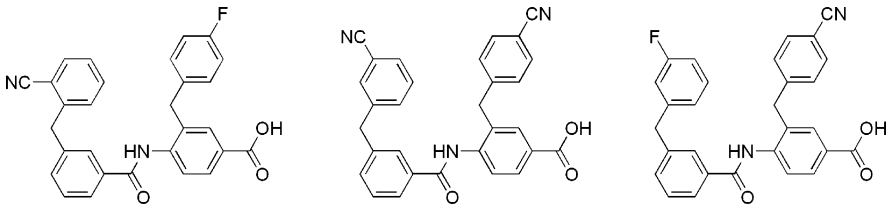

11{7,6} **11**{8,9} **11**{5,9}

Figure 4. Structures of the most potent competitors from chemset **11**.

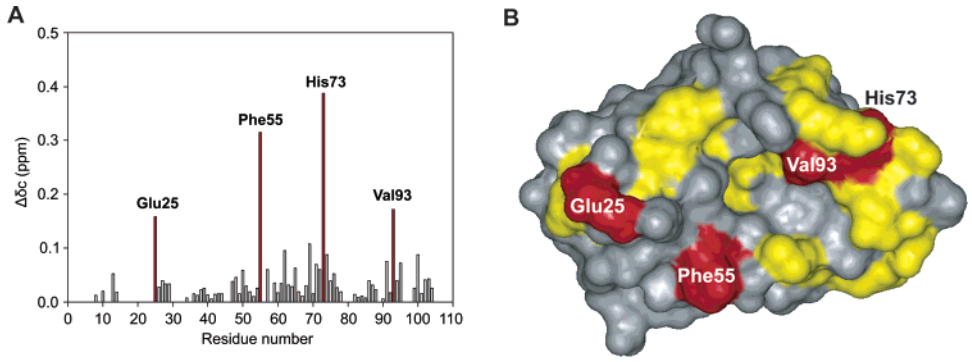

Figure 5. Binding of **11**{*7,6*} to MDM2. (A) Chemical shift perturbation in MDM2 upon binding to 11{*7,6*}. The $\Delta\delta_c(^1H, ^{15}N)$ value was calculated as described earlier[19] when the molar ratio of mdm2 to p53 is 1:0.6. (B) Color-coded structures of mdm2 (3−109) showing the sites of major chemical shift perturbation. The residues showing the major chemical shift perturbation are colored in red on the surface of mdm2 from the crystal structure of mdm2 bound with the p53 peptide.[16] Color-coding is based upon the degree of chemical shift perturbation: gray, $\Delta\delta_c < 0.04$ ppm; yellow, 0.04 ppm $< \Delta\delta_c < 0.15$ ppm; red, $\Delta\delta_c > 0.15$ ppm.

As the first step in the library design process, CAVEAT and its parameters played a large role in determining the scaffold structure. One such parameter is the angle and distance tolerances that describe the allowed deviation from the input structure. These tolerances can be increased or decreased based on the quality of the crystal structure, receptor site flexibility, and desired number of hits. Pilot studies showed a dramatic increase in hits as the tolerance is relaxed. While 11° and 0.24 Å is a conservative margin, larger tolerances would have resulted in too many hits. The bonds chosen for the CAVEAT search are also important. The multitude of options includes other peptide bonds such as the Cβ−Cγ bond and a combination of bonds from nonpeptidic inhibitors. Libraries derived from Cα−Cβ bonds of protein secondary structures have added value because the recurrence of the secondary structures increases the relevance and applicability of the library in other protein−protein interactions. Ultimately, the numerous paths for entering a binding site are equally valid until further investigation and will result in highly varied libraries and inhibitors. Of the four scaffolds we examined closely, one resembled a known MDM2 inhibitor: the chalcone (Figure 1D). The overlap of hits resulting from a screening approach and our computational approach was a significant positive benchmark.

CAVEAT can be classified as a pharmacophore-based modeling program, but it differs from UNITY, the pharmacophore package used in discovery of the norbornane and sulfonamide classes of MDM2 inhibitors. In Galatin and Abraham's search for MDM2 inhibitors, UNITY identifies molecules that contain three pharmacophores described by 19F, 23W, and 26W. Although both programs emphasize the same side chains, UNITY hits incorporate the side chains, while CAVEAT hits only contain the scaffold. As a result, the CAVEAT-based inhibitors are larger, its side chains are easily modified, and the full inhibitor may differ greatly from the original database molecule. Most importantly, the number of hits is dramatically increased with CAVEAT. Searching through the NCI database using a 20% tolerance, UNITY found seven hits. Searching through the NCI database using a much smaller tolerance, CAVEAT found 4000 unique scaffolds.

Because pharmacophore modeling does not account for a molecule's receptor complementarity, it should be used in conjunction with a docking method when a receptor structure is available. Abraham and Galatin checked for receptor clashes in UNITY, Zhao and co-workers used DOCK, and our method also uses several rounds of DOCK scoring. While DOCK was extremely useful in removing molecules with receptor clashes, it would not perform well as the sole tool in a search for inhibitors of a protein−protein interaction. DOCK has successfully identified inhibitors in the past, but these examples have generally used enzyme targets with a small and well-defined binding site. With such a large hydrophobic MDM2 surface, many molecules scoring well in DOCK may not fill the three binding pockets of MDM2. Using CAVEAT compensates for this shortcoming by finding scaffolds that place side chains into the binding pocket.

Library synthesis progressed smoothly after conditions were optimized. The key reaction in the synthesis, which enabled the production of over 100 library members, was the amide bond formation. Two commonly used conditions for amide bond formation include DCC/HOBt or $COCl_2$/DMF/DIEA. The first set of conditions yielded mostly activated ester, and the latter set of conditions gave a 10% purified yield with six products found by thin layer chromatography. Most importantly, the use of oxalyl chloride required anhydrous conditions, a significant obstacle when adapting a reaction for library synthesis. On the other hand, resin-bound TsCl and DMAP effected the transformation quantitatively and did not require anhydrous conditions. As with the liquid form of tosyl chloride, reagent deterioration occurs over a time period of weeks, and it is best to use unopened bottles. This reaction proved to be robust with the majority of missing or failed compounds attributed to tosyl chloride deterioration or human or machine error. It would be feasible to make large libraries using these reaction conditions, with the rate-limiting step being the post-purification fraction sorting and characterization.

Active compounds were members of chemsets **11** and **13**, suggesting that the carboxylic acid functionality serves in an important interaction. To further support this hypothesis, the methyl ester analogue, **10**{*7,6*}, did not have detectable activity. Previous studies have suggested that acidic groups

can disturb the salt bridge between Lys51 and Glu25 of MDM2.[16,19,20] The chemical shift perturbation of Glu25 from the NMR studies indicates that the carboxylic acid group is affecting this salt bridge.

The data also suggests that electron-withdrawing groups are preferred at the para position of the R_2 benzyl ring. Since the R_2 binding pocket is large enough to accommodate a tryptophan group, a meta/para disubstituted benzyl ring in this position may improve binding. A major drawback of the inhibitor library is its hydrophobicity, which posed some solubility problems. Furthermore, with a logP of approximately 10, there is little chance the inhibitor can cross the cell membrane. Two possibilities exist for reducing hydrophobicity and increasing aqueous solubility: the addition of polar side chains to the solvent-exposed face of the inhibitor, and the substitution of scaffold carbons with heteroatoms.

NMR studies indicate that **11**{*7*,*6*} binds to MDM2 in the same pocket in which the p53 helix binds, a result that is consistent with the results of the competitive fluorescence polarization experiments. The most significantly shifted MDM2 residues are Glu25, Phe55, His73, and Val93. These four residues have also shifted during the binding of p53 to MDM2.[19] More specifically, the p53 peptide's Phe19 interacts with His73 of MDM2, and Trp23 of p53 interacts with Val93 of MDM2. Phe55 is a solvent-exposed residue engaging in aromatic interactions with chalcones, and most likely with **11**{*7*,*6*} as well.[19] These results suggest that **11**{*7*,*6*} binds to MDM2 in the Phe19 and Trp23 binding pockets, as the inhibitor design process intended. However, we did not anticipate that a carboxylic acid would play a role in binding or that the leucine pocket was less important for binding. While these structural studies reveal important information, further structural studies are necessary to compare the predicted vs actual binding modes.

We have constructed a library of p53-MDM2 inhibitors, which have a high potential for activity in other protein−protein interactions involving an α-helix. This library represents one of several libraries of compounds targeting an i, $i + 4$, $i + 7$ α-helical system, and the method used for in silico design can be applied to other helical motifs as well as other classes of protein substructures. After creating libraries populating each substructure class, one could screen new protein−protein targets whose binding features have been classified. Thus, recurring protein motifs provide an added advantage by facilitating lead discovery.

Experimental Methods

Inhibitor Design. The structure-based design process began with the coordinates for MDM2 bound to a short segment of p53 (PDB code 1ycr). The Cα−Cβ atoms and bonds of p53 residues 19, 23, and 26 were used as vectors in a CAVEAT search with geometric tolerances of 11° for bond angles and 0.24 Å. The CAVEAT search database containing an average of 10 low-energy conformations of molecules from the combination of the Available Chemicals Directory (ACD), the MDL Drug Data Repository (MDDR), the National Cancer Institute (NCI), comprehensive medicinal chemistry (CMC), Iliad, and Triad was generated using OMEGA (OpenEye).

The 40 000 structures identified by CAVEAT were scored with the DOCK 4.0 van der Waals scoring function. The crystal structure was prepared for docking in a standard manner by removing the p53 peptide and assigning charges by the method of Cornell et al.[41] A 0.15 Å spacing energy grid comprised of a Lennard−Jone 12−6 potential was used to score the rigidly DOCKed molecules. Approximately 10 000 structures scored greater than 1000 and were discarded.

The structures were characterized by two-dimensional Daylight fingerprint descriptors and hierarchically clustered with a closest linkage algorithm using a Tanimoto coefficient of 0.85. Because fingerprint descriptors recognize chemical diversity, all heteroatoms were changed to carbon to effect geometric, rather than chemical, clustering. Of the remaining 761 structures, those with more than six consecutive rotatable bonds or zero rings were removed in a screen for conformational rigidity. Structures with four-membered rings or more than four fused rings were removed due to synthetic difficulty. The application of these filters left 500 remaining clusterheads, which were minimized using DOCK 4.0 scored with a van der Waals scoring function and a narrower cutoff. Conformational variances and heteroatoms were restored to the molecules scoring in the top half, yielding 1369 three-dimensional structures.

Phenylalanine, phenylalanine, and leucine side chains were added to the R_1, R_2, and R_3 positions on the scaffold, corresponding to the 19F, 23W, and 26L positions of p53. These molecules were charged with Gasteiger charges and DOCKed using van der Waals (previously described) and a distance dependent dielectric of 4.[42] The top 250 structures contained approximately 40 unique scaffolds that were considered for library synthesis.

General Synthetic Methods. All reagents and starting materials were purchased from commercial sources and used without further purification; solvents were HPLC grade and degassed and dried with activated alumina. Proofing reactions were carried out in standard glassware, while the production of library intermediates was carried out using Radleys 6- and 12-place reactors. Analytical reverse phase HPLC was performed using an Xterra RPC18 column (3.5 μM, 4.6 × 50 μm, Waters) on an Alliance 2695 HPLC. Preparative reverse phase HPLC was performed using an YMC ODS-AQ column (20 × 50 mm, particle size S-5) on a Parallex Flex HPLC System. MALDI-TOF was carried out with the Voyager-EE STR instrument from Applied Biosystems. Mass spectra were also obtained using a Waters ZQ4000 mass spectrometer with an electrospray probe and single quadrupole detector. ^{1}H NMR were recorded using a Varian 400 MHz spectrometer. Chemical shifts were measured in parts per million (δ) relative to tetramethylsilane as the internal standard. Coupling constants were measured in hertz.

General Procedures for Preparation of Chemset 12. 3-Benzyl-benzaldehyde 2{*1*}. Under argon atmosphere: To a mixture of THF (12.5 mL) and aqueous K_2CO_3 (2 M, 5 mL, 10 mmol) were added 3-formylphenylboronic acid (0.50 g, 3.3 mmol, 1.1 equiv), benzyl bromide (0.36 mL, 3 mmol, 1 equiv), and $Pd(PPh_3)_4$ (0.087 g, 0.075 mmol, 0.025 equiv). The reaction was heated to 80 °C and monitored by periodic

thin layer chromatography (silica, 12:1 hexanes/ethyl acetate, $R_f = 0.3$). Full conversion was reached after 16 h. The reaction was quenched with aqueous HCl (1 M, 50 mL), and the aqueous phase was extracted with ethyl acetate (3 × 30 mL). The combined organic layers were dried using $MgSO_4$, and solvent was removed in vacuo giving the crude product. The crude material was purified by flash chromatography [silica gel, hexanes/ethyl acetate (12:1)] to give 0.5 g (80%) of the product. ^{1}H NMR (400 MHz, $CDCl_3$): $\delta =$ 9.98 (s, 1H), $\delta = 7.723$ (m, 1H), $\delta = 7.459$ (d, $J = 5.6$ Hz, 1H), $\delta = 7.26$ (m, 7H), $\delta = 4.062$ (s, 2H).

3-Benzyl-benzoic Acid 3{*1*}. An aqueous solution of $NaClO_2$ (3.5 M, 4 mL, 14 mmol, 7 equiv) was added dropwise in 1 h to a stirred mixture of 3-benzyl-benzaldehyde (0.39 g, 2.0 mmol, 1 equiv), aqueous NaH_2PO_4 (0.7 M, 7 mL, 4.9 mmol, 2.5 equiv), and 35% H_2O_2 (1 mL, 10 mmol, 5 equiv) in acetonitrile (15 mL), keeping the temperature below 10 °C using an ice bath. After the addition was complete, the ice bath was removed and the reaction was monitored by periodic thin layer chromatography following the disappearance of starting material (silica, 12:1 hexanes/ethyl acetate, $R_f = 0$). In 2 h, the reaction had proceeded to completion and sodium sulfite (1.8 g, 14 mmol, 7 equiv) was added to quench the reaction. The solution was acidified with aqueous HCl to pH 3 as indicated using pH paper. The organic phase was separated and dried in vacuo to afford 0.54 g (75%) of the product. ^{1}H NMR (400 MHz, $CDCl_3$): $\delta = 7.95$ (m, 2H), $\delta = 7.41$ (m, 2H), $\delta = 7.25$ (m, 5H), $\delta = 6.65$ (bs, 1H), $\delta = 4.046$ (s, 2H).

2-Benzyl-nitrobenzene 8{*1*}. Under argon atmosphere: To a mixture of THF (12.5 mL) and aqueous K_2CO_3 (2 M, 5 mL, 10 mmol) were added 2-nitrophenylboronic acid (0.55 g, 3.3 mmol, 1.1 equiv), benzyl bromide (0.36 mL, 3 mmol, 1 equiv), and $Pd(PPh_3)_4$ (0.087 g, 0.075 mmol, 0.025 equiv). The reaction was heated to 80 °C and monitored by periodic thin layer chromatography (silica, 12:1 hexanes/ethyl acetate, $R_f = 0.4$). Full conversion was reached after 16 h. The reaction was quenched with HCl (1 M, 50 mL), and the aqueous phase was extracted with ethyl acetate (3 × 30 mL). Solvent was removed in vacuo giving the crude product. The crude material was purified by flash chromatography [silica gel, hexanes/ethyl acetate (12:1)] to give 0.22 g (33%) of the product. ^{1}H NMR (400 MHz, $CDCl_3$): $\delta = 7.932$ (dd, $J = 8$,1.4 Hz, 1H), $\delta = 7.512$ (td, $J = 7.6$, 1.2 Hz, 1H), $\delta = 7.375$ (td, $J = 7.6$,1.2 Hz, 1H), $\delta = 7.4$ (m, 6H), $\delta =$ 4.312 (s, 2H).

2-Benzyl-phenylamine 9{*1*}. Under hydrogen atmosphere: 10% palladium on carbon (20 mg, 50% wet) was added to a solution of 2-benzyl-nitrobenzene (0.22 g, 1 mmol) in MeOH (15 mL). The reaction was conducted using a Parr apparatus under 30 psi of H_2. Full conversion was reached after 1 h, as indicated by thin layer chromatography (silica, 12:1 hexanes/ethyl acetate, $R_f = 0.3$). The mixture was filtered, and the solvent was removed in vacuo to afford 0.16 g (87%) of the product. ^{1}H NMR (400 MHz, $CDCl_3$): $\delta =$7.4 (m, 6H), $\delta = 6.768$ (td, $J = 7.6$, 1.2 Hz, 1H), $\delta =$ 6.678 (d, $J = 8$ Hz), $\delta = 3.908$ (s, 2H), $\delta = 3.5$ (bs, 2H).

4-Amino-3-(4,4,5,5-tetramethyl-[1,3,2]dioxaborolan-2-yl)-benzoic Acid Methyl Ester (5). Under argon atmosphere: To a mixture of methyl 4-amino-3-iodo-benzoate (2.3 g, 8.2 mmol, 1 equiv) in 1,4-dioxane (20 mL), triethylamine (4.6 mL, 33 mmol, 4 equiv), and $PdCl_2$(dppf) (0.30 g, 0.4 mmol, 0.005 equiv) was added pinacolborane (3.6 mL, 25 mmol, 3 equiv) dropwise at room temperature. The reaction was heated to 80 °C and monitored by thin layer chromatography (silica, dichloromethane, $R_f = 0.1-$ 0.5). Full conversion was reached after 8 h. The reaction was slowly quenched with aqueous saturated NH_4Cl (30 mL), and the aqueous phase was extracted with diethyl ether (7 × 25 mL). After drying over $MgSO_4$, the solution was filtered over a patch of silica. Subsequently the silica was washed with methylene chloride (1 L). Concentration of the solution in vacuo gave 0.49 g of a mixture of the product and methyl-4-aminobenzoate. ^{1}H NMR (400 MHz, $CDCl_3$): $\delta = 8.310$ (d, $J = 2$ Hz, 1H), $\delta = 7.888$ (d, $J = 2.4$ Hz, 1H), $\delta = 6.551$ (d, $J = 8.8$ Hz, 1H), $\delta = 3.844$ (s, 3H), $\delta = 5.184$ (bs, 2H), $\delta = 1.346$ (s, 12H).

Methyl 4-Amino-3-benzyl-benzoate 6{*1*}. Under argon atmosphere: To a mixture of THF (8 mL) and aqueous K_2CO_3 (2 M, 1.6 mL, 3.2 mmol) were added crude 4-amino-3-(4,4,5,5-tetramethyl-[1,3,2]dioxaborolan-2-yl)-benzoic acid methyl ester (0.49 g,1.8 mmol, 1 equiv), benzyl bromide (0.40 mL, 3.6 mmol, 2 equiv), and $Pd(PPh_3)_4$ (0.050 g, 0.043 mmol, 0.025 equiv). The reaction was heated to 80 °C and monitored by TLC (silica, dichloromethane, $R_f = 0.4$). The reaction was quenched with aqueous HCl (1 M, 50 mL), and the aqueous phase was extracted with ether (3 × 30 mL). Solvent was removed in vacuo from the combined organic layers. The crude material was purified by flash chromatography [silica gel, dichloromethane/hexanes (5:1)] to give 0.1 g (20%) of the product. ^{1}H NMR (400 MHz, $CDCl_3$): $\delta = 7.81$ (m, 2H), $\delta = 7.2$ (m, 5H), $\delta = 6.634$ (d, $J = 8.4$ Hz, 1H), $\delta =$3.930 (s, 2H), $\delta = 3.898$ (bs, 2H), $\delta =$3.860 (s, 3H).

Methyl 4-Amino-3-benzyl-benzoate 6{*1*}. Under argon atmosphere: To a mixture of methyl 4-amino-3-iodo-benzoate (2.27 g, 8.19 mmol, 1 equiv) in 1,4-dioxane (20 mL), triethylamine (4.6 mL, 33 mmol, 4 equiv), and $PdCl_2$-(dppf) (0.30 g, 0.4 mmol, 0.005 equiv) was added pinacolborane (3.6 mL, 25 mmol, 3 equiv) dropwise at room temperature. After 16 h at 80 °C, benzyl bromide (0.9 mL, 8 mmol, 1 equiv), aqueous K_2CO_3 (2 M, 6.3 mL, 13 mmol), and $Pd(PPh_3)_4$ (0.22 g, 0.19 mmol, 0.02 equiv) were added. After 24 h, the reaction was quenched with saturated NH_4-Cl and the aqueous phase was extracted with ethyl acetate. Solvent was removed in vacuo from the combined organic layers. The crude material was purified by flash chromatography [silica gel, dichloromethane/hexanes (5:1)] to give 0.7 g (35%) of the product.

3-Benzyl-4-(3-benzyl-benzoylamino)-benzoic Acid Methyl Ester 10{*1,1*}. Under argon atmosphere: To a mixture of 3-benzyl-benzoic acid (0.21 g, 1 mmol, 1 equiv), DMAP (0.49 g, 4 mmol, 4 equiv), and PS-TsCl (1.0 g, 1.5 mmol, 1.5 equiv) were added methylene chloride (15 mL) and methyl 4-amino-3-benzyl-benzoate (0.24 g, 1 mmol, 1 equiv). The reaction was heated to 40 °C and monitored by thin layer chromatography (silica, 10:1 hexanes/ethyl acetate, $R_f = 0.3$). The crude material was filtered and purified by flash chromatography [silica gel, hexanes/ethyl acetate (10:1)] to

give 0.39 g (90%) of the product. ^{1}H NMR (400 MHz, $CDCl_3$): $\delta = 8.371$ (d, $J = 9.2$, 1H), $\delta = 8.04$ (m, 2H), $\delta = 7.745$ (s, 1H), $\delta = 7.4$ (m, 1H), $\delta = 7.2$ (m, 11H), $\delta = 6.994$ (d, $J = 6.8$, 1H), $\delta = 3.954$ (s, 3H), $\delta = 3.948$ (s, 2H), $\delta = 3.843$ (s, 2H).

3-Benzyl-4-(3-benzyl-benzoylamino)-benzoic Acid 11-{*1,1*}. To 3-benzyl-4-(3-benzyl-benzoylamino)-benzoic acid methyl ester (0.35 g, 0.8 mmol, 1 equiv) was added a 4:1 solution of THF/MeOH until the ester became soluble (30−50 mL). Aqueous NaOH (12 mL, 50% w/v) was added to the solution, and the reaction was monitored by thin layer chromatography (silica, 20:1 dichloromethane/acetic acid, $R_f = 0.2$). Full conversion was reached after 72 h, and the reaction was quenched with 6 M HCl to pH 3, as indicated by pH paper. The quenched reaction was extracted with dichloromethane (3 × 30 mL), and the solvent was removed in vacuo from the combined organic layers. The crude material was purified by flash chromatography [silica gel, dichloromethane/acetic acid (20:1)] to give 0.30 g (90%) of the product. ^{1}H NMR (400 MHz, d_6-DMSO): $\delta = 9.884$ (s, 1H), 7.774 (d, $J = 8.4$, 1H), $\delta = 7.714$ (s, 1H), $\delta = 7.58$ (m, 4 H), $\delta = 7.38$ (m, 2 H), $\delta = 7.2$ (m, 8 H), $\delta = 4.049$ (s, 2H), $\delta = 3.958$ (s, 2H); MS calcd for $C_{28}H_{23}NO_3$ 421.17, found 422.48.

12{*1,1,1*}. These reactions were carried out in parallel in polypropylene fritted FlexChem 48-well reaction blocks rotating at 700 rpm. To a mixture of 3-benzyl-4-(3-benzyl-benzoylamino)-benzoic acid (17 mg, 0.04 mmol, 1 equiv), DMAP (20 mg, 0.16 mmol, 4 equiv), and PS-TsCl (40 mg, 0.06 mmol, 1.5 equiv) were added DMF (2 mL) and 2-benzyl-phenylamine (7.3 mg, 0.04 mmol, 1 equiv). After 72 h at 40 °C the reaction was filtered and purified by reverse phase HPLC (see purification procedure below) to give 14 mg (60%) of the product. ^{1}H NMR (400 MHz, d_6-DMSO): $\delta = 9.927$ (s, 1H), $\delta = 9.858$ (s, 1H), $\delta = 7.750$ (m, 2H), $\delta = 7.689$ (s, 1H), $\delta = 7.658$ (d, $J = 6.8$, 1H), $\delta = 7.559$ (d, $J = 8.0$, 1H), $\delta = 7.3$ (m, 21H), $\delta = 4.099$ (s, 1H), $\delta = 4.011$ (s, 2H); HRMS calcd for $C_{41}H_{34}N_2O_2$ 586.2620, found 587.2708.

General Procedure for Purification of Chemset 12. The crude compounds in a solution of DMF were purified with a preparative YMC ODS-AQ column (20 × 50 mm, particle size S-5) running a 5−95% gradient of acetonitrile/0.05% trifluoracetic acid with a 20 mL/min flow rate on a Parallex Flex HPLC System. Chromatographs were monitored with a dual wavelength UV detector at 220 and 254 nm. Fraction collection was automatically triggered by UV absorption above 0.05 AU at either wavelength. All fractions eluted with 50% acetonitrile or greater were analyzed with an Xterra RPC18 column (3.5 uM, 4.6 × 50 μm, Waters) running a 0−100% gradient of acetonitrile/0.05% trifluoroacetic acid with a 1 mL/min flow rate on a Alliance 2695 HPLC (Waters). Peaks were integrated at 254 nm using Millenium software (Waters). Samples with 95% purity or greater were further characterized by MALDI-TOF (Voyager-EE STR, Applied Biosystems). Fractions containing the correct product of 95% purity or greater were pooled. Pooled fractionswere dried down using a GeneVac Mega 980 solvent evaporator.

General Procedures for Preparation and Purification of Chemsets 11 and 13. 3-Benzyl-4-(3-benzyl-benzoylamino)-benzoic Acid Methyl Ester 10{*1,1*}. These reactions were carried out in parallel in polypropylene fritted FlexChem 48-well reaction blocks rotating at 700 rpm. To a mixture of 3-benzyl-benzoic acid (0.02 g, 0.1 mmol, 1 equiv), DMAP (50 mg, 0.4 mmol, 4 equiv), and PS-TsCl (100 mg, 0.15 mmol, 1.5 equiv) were added DMF (2 mL) and methyl 4-amino-3-benzyl-benzoate (0.02 g, 0.1 mmol, 1 equiv). After 48 h at 40 °C, the crude reaction was filtered and purified on a Parallex Flex HPLC System as described above. All fractions eluted with 30% acetonitrile or greater were characterized by LC/MS using an Alliance 2695 HPLC and Waters ZQ4000 mass spectrometer with an electrospray probe and single quadrupole detector operating in positive ion mode. Fractions containing the correct product of 30% purity or greater were pooled and dried down using a GeneVac Mega 980 solvent evaporator.

3-Benzyl-4-(3-benzyl-benzoylamino)-benzoic Acid 11-{*1,1*}. These reactions were carried out in parallel in glass test tubes rested in FlexChem 48-well reaction blocks rotating at 300 rpm. To the pooled fractions from the previous reaction was added 2 mL of 15:1 solution of dioxane/50% NaOH. Full conversion was reached after 72 h, and the reaction was quenched with HCl (6 M, 2 mL, 12 mmol). The quenched reaction was extracted with dichloromethane (2 × 2 mL). The crude material was purified on a Parallex Flex HPLC System as described above. All fractions eluted with 50% acetonitrile or less were characterized by LC/MS using an Alliance 2695 HPLC and Waters ZQ4000 mass spectrometer with an electrospray probe and single quadrupole detector operating in positive ion mode. Fractions containing the correct product of 95% purity or greater were pooled and dried down using a GeneVac Mega 980 solvent evaporator.

Recombinant MDM2. Plasmid encoding His-hDM2 (1−222) was kindly donated by R. Tjian.[43] Protein was expressed in BL21(DE3) RAI cells (Stratagene) grown at 37 °C to $OD_{600} = 0.6$ and induced for 3 h under 1 mM β-D-thiogalactopyranoside. The cells were harvested, sonicated, and centrifuged at 35000*g* for 15 min. The supernatant was loaded onto Ni−NTA resin and eluted with 250 mM imidazole. The protein was further purified by ion exchange chromatography using a Source 15Q column (20 mM Tris-HCl, pH 8.0, 1 mM DTT, 110 mM NaCl) and quantified by Coomassie protein assay.

Peptides. The following peptides were synthesized on an Applied Biosystems Model 433A peptide synthesizer using Fmoc chemistry: GSGSSQETFSDLWKLLPEN, GSGSSQETASDLAKLAPEN. TFA cleavage was performed using Reagent K, as described by Method 3-18, "General TFA Cleavage", in the 2004/5 Novabiochem catalog. The peptides were isolated according to Method 3-29, "Post-Cleavage Work-up", in the 2004/5 Novabiochem catalog. Peptides were purified using the Parallex Flex HPLC System as described above.

p53−FITC. To aqueous $NaHCO_3$ (0.2 M, 0.5 mL, 0.1 mmol, pH 7.0) were added p53 peptide (2 mg, 1 μmol, 1 equiv) and FITC (Molecular Probes) (50 mM in DMF, 100

μL, 5 μmol, 5 equiv). These reaction conditions are also described in "Amine-Reactive Probes", product information distributed by Molecular Probes. The reaction was monitored on a Alliance 2695 HPLC (Waters) running a 0−100% gradient of acetonitrile/0.05% trifluoroacetic acid with a 1 mL/min flow rate. Because the p53 peptide contains lysine, the low pH and reaction time were important to ensure labeling at a single site. Full conversion was achieved after 4 h, and the crude material was purified using the Parallex Flex HPLC System as described above.

Assays. Measurements were made with an LJL Biosystems Analyst AD plate reader using a 485 nM excitation filter and a 535 nM emission filter. Assays were performed in Corning 384-well black plates. Pilot experiments demonstrated that the binding of p53−FITC was saturable, and our observed K_d agreed well with the reported value of 2 μM. Nutlin-3 (Cayman Chemicals) was used as a positive control, while both DMSO and p53 peptide with alanine substitutions at 19F, 23W, and 26L were used as negative controls. Assays were performed in duplicate and repeated at least twice on separate days with different batches of protein. Competition experiments were carried out in a total volume of 20 μL 40 mM Tris-HCl, pH 8.0, 150 mM NaCl, 1 mM DTT, 5% DMSO, and 0.05% Tween 20. Probe peptide was present at a final concentration of 10 nM, and MDM2 was present at a final concentration of 2 μM. Plates were allowed to incubate at room temperature for 1 h prior to measurement. Data were analyzed with SigmaPlot.

NMR Spectroscopy. NMR spectra were acquired using a Varian Unity INOVA 600 spectrometer equipped with a cold probe. NMR samples contained 0.1 mM ^{15}N-labeled MDM2 (amino acid residues 3−109) in 90% H_2O/10% H_2O, 25 mM TrisHCl (pH 7.5), 150 mM NaCl, 2 mM DTT, 0.1 mM PMSF, 0.1 mM EDTA, 0.1 mM benzamidine, and 0.02% NaN_3. Aliquots of **11**{*7,6*} were added in a stepwise fashion to the ^{15}N-labeled MDM2 (3−109) during titration. The ^{15}N-^{1}H HSQC spectra were collected for the unbound mdm2 (3−109) alone or with **11**{*7,6*} at 25 °C. The final molar ratio of MDM2 to **11**{*7,6*} was 1:1. The resonance assignment of MDM2 (3−109) was previously obtained (accession number 2410, BioMagResBank).[44] For some residues assignment was confirmed under the particular NMR solution condition used (K. Han, unpublished results).

Acknowledgment. This work was supported by National Institutes of Health Grants GM 56531 (P. Ortiz de Montellano) and DK 58080 (R.K.G.) and technology development grants from the Sandler Research Foundation (R.K.G.). We thank Nathan Sallee, Brian Yeh, and the Wendell Lim laboratory for their help with MDM2 synthesis and purification and Andrew Finch, Abigail Hunt, and the Gerard Evan lab for their help with cellular assays.

Supporting Information Available. Tables of yield and purity data for all compounds; tabulated complete screening data; ^{1}H NMR, HPLC, and MS spectra for 20 library members; and OMEGA, DOCK, and CAVEAT parameters. This material is available free of charge via the Internet at http://pubs.acs.org.

References and Notes

(1) Kuntz, I. D.; Chen, K.; Sharp, K. A.; Kollman, P. A. *Proc. Natl. Acad. Sci. U.S.A.* **1999**, *96* (18), 9997−10002.
(2) Fairlie, D. P.; West, M. L.; Wong, A. K. *Curr. Med. Chem.* **1998**, *5* (1), 29−62.
(3) Pagliaro, L.; Felding, J.; Audouze, K.; Nielsen, S. J.; Terry, R. B.; Krog-Jensen, C.; Butcher, S. *Curr. Opin. Chem. Biol.* **2004**, *8* (4), 442−449.
(4) Toogood, P. L. *J. Med. Chem.* **2002**, *45* (8), 1543−1558.
(5) Berg, T. *Angew. Chem., Int. Ed.* **2003**, *42* (22), 2462−2481.
(6) Orner, B. P.; Ernst, J. T.; Hamilton, A. D. *J. Am. Chem. Soc.* **2001**, *123* (22), 5382−5383.
(7) Ernst, J. T.; Becerril, J.; Park, H. S.; Yin, H.; Hamilton, A. D. *Angew. Chem., Int. Ed.* **2003**, *42* (5), 535−539.
(8) Ernst, J. T.; Kutzki, O.; Debnath, A. K.; Jiang, S.; Lu, H.; Hamilton, A. D. *Angew. Chem., Int. Ed.* **2001**, *41* (2), 278−+.
(9) Yin, H.; Hamilton, A. D. *Bioorg. Med. Chem. Lett.* **2004**, *14* (6), 1375−1379.
(10) Yin, H.; Lee, G. I.; Park, H. S.; Payne, G. A.; Rodriguez, J. M.; Sebti, S. M.; Hamilton, A. D. *Angew. Chem., Int. Ed.* **2005**, *44* (18), 2704−2707.
(11) Anderson, A. C. *Chem. Biol.* **2003**, *10* (9), 787−797.
(12) Bogan, A. A.; Thorn, K. S. *J. Mol. Biol.* **1998**, *280* (1), 1−9.
(13) Kortemme, T.; Baker, D. *Proc. Natl. Acad. Sci. U.S.A.* **2002**, *99* (22), 14116−14121.
(14) Levine, A. J. *Cell* **1997**, *88* (3), 323−331.
(15) Momand, J.; Jung, D.; Wilczynski, S.; Niland, J. *Nucleic Acids Res.* **1998**, *26* (15), 3453−3459.
(16) Kussie, P. H.; Gorina, S.; Marechal, V.; Elenbaas, B.; Moreau, J.; Levine, A. J.; Pavletich, N. P. *Science* **1996**, *274*, 948−953.
(17) Bottger, A.; Bottger, V.; Howard, S. F.; Picksley, S. M.; Chene, P.; Garcia-Echeverria, C.; Hochkeppel, H. K.; Lane, D. P. *Oncogene* **1996**, *13*, 2141−2147.
(18) Garcia-Echeverria, C.; Chene, P.; Blommers, M. J. J.; Furet, P. *J. Med. Chem.* **2000**, *43* (17), 3205−3208.
(19) Stoll, R.; Renner, C.; Hansen, S.; Plame, S.; Klein, C.; Belling, A.; Zeslawski, W.; Kamionka, M.; Rehm, T.; Muhlhahn, P.; Schumacher, R.; Hesse, F.; Kaluza, B.; Voelter, W.; Engh, R.; Holak, T. *Biochemistry* **2001**, *40*, 336−344.
(20) Kumar, S. K.; Hager, E.; Pettit, C.; Gurulingappa, H.; Davidson, N. E.; Khan, S. R. *J. Med. Chem.* **2003**, *46* (14), 2813−2815.
(21) Luke, R. W. A.; Jewsbury, P. J.; Cotton, R. Piperizine-4-phenyl derivatives as inhibitors of the interaction between MDM2 and p53. PCT Int. Appl., 2000.
(22) Duncan, S. J.; Gruschow, S.; Williams, D. H.; McNicholas, C.; Purewal, R.; Hajek, M.; Gerlitz, M.; Martin, S.; Wrigley, S. K.; Moore, M. *J. Am. Chem. Soc.* **2001**, *123* (4), 554−560.
(23) Zhao, J.; Wang, M.; Chen, J.; Luo, A.; Wang, X.; Wu, M.; Yin, D.; Liu, Z. *Cancer Lett.* **2002**, *183*, 69−77.
(24) Vassilev, L. T.; Vu, B. T.; Graves, B.; Carvajal, D.; Podlaski, F.; Filipovic, Z.; Kong, N.; Kammlott, U.; Lukacs, C.; Klein, C.; Fotouhi, N.; Liu, E. A. *Science* **2004**, *303* (5659), 844−848.
(25) Galatin, P. S.; Abraham, D. J. *J. Med. Chem.* **2004**, *47* (17), 4163−4165.
(26) Grasberger, B. L.; Lu, T. B.; Schubert, C.; Parks, D. J.; Carver, T. E.; Koblish, H. K.; Cummings, M. D.; LaFrance, L. V.; Milkiewicz, K. L.; Calvo, R. R.; Maguire, D.; Lattanze, J.; Franks, C. F.; Zhao, S. Y.; Ramachandren, K.; Bylebyl, G. R.; Zhang, M.; Manthey, C. L.; Petrella, E. C.; Pantoliano, M. W.; Deckman, I. C.; Spurlino, J. C.; Maroney, A. C.; Tomczuk, B. E.; Molloy, C. J.; Bone, R. F. *J. Med. Chem.* **2005**, *48* (4), 909−912.

(27) Hardcastle, I. R.; Ahmed, S. U.; Atkins, H.; Calvert, A. H.; Curtin, N. J.; Farnie, G.; Golding, B. T.; Griffin, R. J.; Guyenne, S.; Hutton, C.; Kallbad, P.; Kemp, S. J.; Kitching, M. S.; Newell, D. R.; Norbedo, S.; Northen, J. S.; Reid, R. J.; Saravanan, K.; Willems, H. M. G.; Lunec, J., *Bioorg. Med. Chem. Lett.* **2005**, *15* (5), 1515−1520.
(28) Lauri, G.; Bartlett, P. A. *J. Comput-Aided Mol. Des.* **1994**, *8*, 51−66.
(29) MDL Information Systems: www.mdli.com.
(30) National Cancer Institute. cactus.nci.nih.gov/ncidb/download.html.
(31) Ewing, T. J. A.; Makino, S.; Skillman, A. G.; Kuntz, I. D. *J. Comput-Aided Mol. Des.* **2001**, *15* (5), 411−428.
(32) Willett, P. *Similarity and Clustering in Chemical Information Systems*; John Wiley & Sons: New York, 1987; p 266.
(33) Greenbaum, D. C.; Arnold, W. D.; Lu, F.; Hayrapetian, L.; Baruch, A.; Krumrine, J.; Toba, S.; Chehade, K.; Bromme, D.; Kuntz, I. D.; Bogyo, M. *Chem. Biol.* **2002**, 9 (10), 1085−1094.
(34) Klarner, C.; Greiner, A. *Macromol. Rapid Commun.* **1998**, *19*, 605−608.
(35) Dalcanale, E.; Montanari, F. *J. Org. Chem.* **1986**, *51*, 567−569.
(36) Seaman, W.; Johnson, J. R. *J. Am. Chem. Soc.* **1931**, *53*, 711−723.
(37) Baudoin, O.; Guenard, D.; Gueritte, F. *J. Org. Chem.* **2000**, *65* (26), 9268−9271.
(38) Ueki, H.; Ellis, T. K.; Martin, C. H.; Boettiger, T. U.; Bolene, S. B.; Soloshonok, V. A. *J. Org. Chem.* **2003**, *68* (18), 7104−7107.
(39) Knight, S. M. G.; Umezawa, N.; Lee, H. S.; Gellman, S. H.; Kay, B. K. *Anal. Biochem.* **2002**, *300* (2), 230−236.
(40) Zhang, R. M.; Mayhood, T.; Lipari, P.; Wang, Y. L.; Durkin, J.; Syto, R.; Gesell, J.; McNemar, C.; Windsor, W. *Anal. Biochem.* **2004**, *331* (1), 138−146.
(41) Cornell, W. D.; Cieplak, P.; Bayly, C. I.; Gould, I. R.; Merz, K. M.; Ferguson, D. M.; Spellmeyer, D. C.; Fox, T.; Caldwell, J. W.; Kollman, P. A. *J. Am. Chem. Soc.* **1995**, *117*, 5179.
(42) Gasteiger, J.; Marsili, M. *Tetrahedron* **1980**, *36*, 3219−3288.
(43) Thut, C. J.; Goodrich, J. A.; Tjian, R. *Genes Dev.* **1997**, *11* (15), 1974−1986.
(44) Stoll, R.; Renner, C.; Muhlhahn, P.; Hansen, S.; Schumacher, R.; Hesse, F.; Kaluza, B.; Engh, R. A.; Voelter, W.; Holak, T. A. *J. Biomol. NMR* **2000**, *17* (1), 91−92.

CC050142V